Electronic properties of the metastable defect in boron-doped Czochralski silicon: Unambiguous determination by advanced lifetime spectroscopy

S. Rein[a] and S. W. Glunz
Fraunhofer Institute for Solar Energy Systems (ISE), Heidenhofstrasse 2, D-79110 Freiburg, Germany

(Received 12 September 2002; accepted 17 December 2002)

By combining data from temperature- and injection-dependent lifetime spectroscopy (TDLS and IDLS) measured by means of the microwave-detected photoconductance decay technique and the quasi-steady state photoconductance technique, respectively, the exact electronic structure of the metastable defect in standard boron-doped Czochralski (Cz) silicon has been determined. A detailed Shockley–Read–Hall analysis of the entire TDLS curve reveals that the Cz-specific defect acts as an attractive Coulomb center [$\sigma_n(T)=\sigma_{n0}T^{-2}$] which is localized in the upper band-gap half at $E_C-E_t=0.41$ eV and has an electron/hole capture cross section ratio $k=\sigma_n/\sigma_p=9.3$. The accuracy of this determination manifests itself by the fact that the corresponding IDLS curve can be simulated with the same parameter set. © *2003 American Institute of Physics.* [DOI: 10.1063/1.1544431]

It is well known that minority carrier lifetime in boron-doped and oxygen-contaminated Czochralski-grown silicon (Cz-Si) is limited by a metastable defect which can be activated by carrier injection and deactivated by a thermal treatment at around 200 °C.[1–4] Up to now, all known properties of the Cz-specific defect have been determined by means of lifetime spectroscopy (LS),[5] which is based on the general Shockley–Read–Hall (SRH) theory,[6,7] as it was not possible to detect the defect, e.g., by deep-level transient spectroscopy (DLTS). Nevertheless, the exact electronic structure of the Cz defect in its active state, which is given by the energy level E_t and the ratio $k=\sigma_n/\sigma_p$ of the capture cross section for electrons and holes, is still unknown. While injection-dependent lifetime spectroscopy (IDLS) only allowed the determination of an energy range between $E_V+0.35$ and $E_C-0.45$ eV for the energy level E_t,[2] temperature-dependent lifetime spectroscopy (TDLS) was restricted to the determination of an upper limit of 0.41 eV for the energy depth ΔE_t from either band edge since only the slope of the linear Arrhenius increase was evaluated.[3] Recently, Rein *et al.*[8] have demonstrated that a modeling of the entire TDLS curve *often* allows an unambiguous determination of the symmetry factor $k=\sigma_n/\sigma_p$ and provides the additional information about the band-gap half. Furthermore, it has been shown that lifetime spectroscopy *always* allows a complete defect characterization if TDLS and IDLS data, measured on the same sample, are combined.[8] Excellent agreement between LS and DLTS has been achieved on intentionally metal-contaminated silicon samples.[8]

The focus of this work is to apply this advanced LS analysis to TDLS and IDLS data obtained by means of the contactless microwave-detected photoconductance decay technique (MWPCD)[5] and the quasi-steady-state photoconductance technique (QSSPC),[9] respectively, on standard *p*-type boron-doped Cz-Si samples with different boron and oxygen concentration. While the oxygen concentration was determined by means of infrared spectroscopy, the doping concentration was determined by means of a resistance measurement based on the four-point-probe technique. In order to minimize surface recombination, the samples were first damage etched in an acid etch and then coated on both sides with silicon nitride which leads to surface recombination velocities below 20 cm/s in the whole injection range.[10]

The TDLS analysis of the Cz-specific defect in its active state faces the problem that the E_t-dominated Arrhenius increase of carrier lifetime due to SRH statistics is superposed by an increase due to defect annihilation, as both effects occur in the same temperature range.[3] Thus a fundamental prerequisite for a direct determination of E_t by TDLS is an efficient suppression of defect annihilation. For this the sample is fully degraded by an illumination step of 36 h under a xenon lamp (intensity 100 mW/cm^2, ~AM1.5) prior to the TDLS measurement and then illuminated with a maximum degradation light of 300 mW/cm^2 between subsequent lifetime measurements during temperature ramping-up. In order to control a possible defect annihilation precisely, the sample is kept on each temperature step for 15 min while being illuminated with 300 mW/cm^2. Lifetime measurements repeated once a minute allows to observe the defect transformation kinetics. To guarantee low injection conditions (LLI) of the TDLS curve, the lifetime measurements themselves are performed at the minimum bias light intensity excluding trapping effects (for details see Ref. 5). Up to 460 K (187 °C), the lifetime series on each temperature step exhibits no systematic increase, which indicates the complete suppression of defect annihilation by the applied bias light. As an overcompensation of defect annihilation fails above 475 K (202 °C), the temperature ramping-up is performed as quickly as possible from 475 to 520 K only allowing one single lifetime measurement at each temperature step. The experiment reveals a critical parameter: especially for higher temperatures the measured carrier lifetime strongly depends on the delay, in the order of a few seconds, between switching off the degradation light and the lifetime measurement under LLI conditions. In order to reduce this systematic error in the lifetime measurement, we averaged over the five smallest lifetimes selected from the 15 measurements taken

[a]Electronic mail: rein@ise.fhg.de

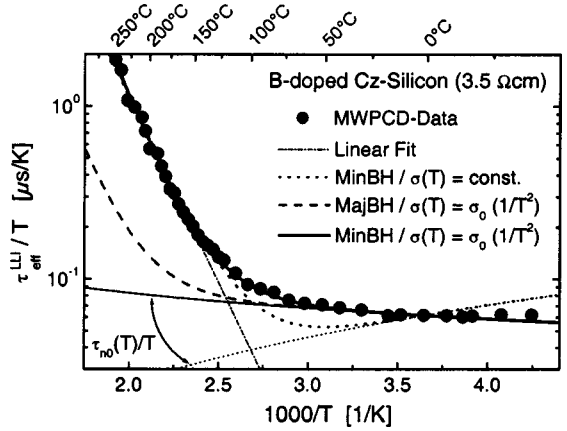

FIG. 1. TDLS curve measured by means of the MW PCD-method on a standard boron-doped Cz-sample with $N_a = 4.0 \times 10^{15}$ cm^{-3} and $[O_i] = 1.0 \times 10^{18}$ cm^{-3} after degradation under AM1.5 (intensity 100 mW/cm^2) at 25 °C for 36 h (closed circles). An accurate SRH simulation (solid line) of the TDLS curve is only achieved for a MinBH-defect in the upper band-gap half and requires the insertion of a temperature-dependent capture cross section, which is reflected in the shape of the electron capture time $\tau_{n0}(T) \propto 1/\sigma_n(T)$ (thin dotted and thin solid line).

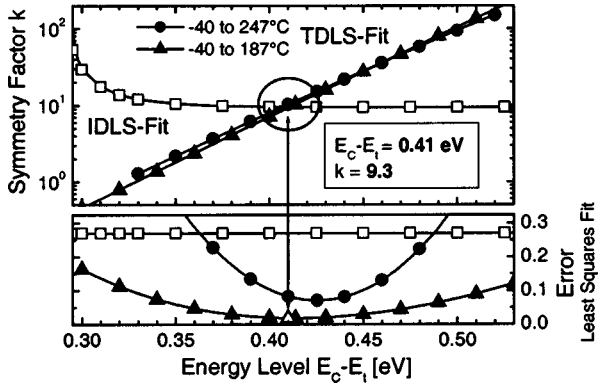

FIG. 2. Defect parameter solution surface (DPSS): The displayed symmetry factors $k_{opt}(E_C - E_t)$ (upper half) are defined in a way that they are leading to the smallest possible least squares errors (lower half) when the SRH simulation of the investigated TDLS (closed symbols) or IDLS (open symbols) curve is performed for the given energy level $E_C - E_t$.

within each 15 min series. The resulting TDLS curve, which represents the active state of the Cz-specific defect, is displayed in Fig. 1.

The observation that an overcompensation of the defect annihilation can be achieved within a broad temperature range is supported by the findings of a quantitative comparison of the kinetics of defect formation and annihilation with data published recently: both processes seem to be thermally activated.[3,4] While the defect annihilation rates $R_{ann}(T)$ were investigated from 380 to 420 K,[3,4] Schmidt *et al.* investigated the defect generation rates $R_{gen}(T)$ from 300 to 350 K.[4] Only for a 1.1 Ω cm sample *both* curves were determined.[4] An extrapolation of the measured $R_{gen}(T)$ into the temperature range up to 450 K shows that $R_{gen}(T)$ surmounts $R_{ann}(T)$ up to a temperature of 425 K (152 °C), which is given by the intersection point of both curves. The higher temperature of 460 K (187 °C) observed for the intersection point in the present work most likely results from the lower doping concentration of the investigated 3.5 Ω cm sample.

The SRH analysis performed on the TDLS curve is displayed in Fig. 1. If just the slope of the linear Arrhenius increase (dash–dotted line) is evaluated, as done in all previous works, an energy depth $\Delta E_t = 0.426$ eV is determined in consistence with former results. If the entire TDLS curve is simulated, the dotted line shows that a standard SRH fit with temperature-independent capture cross sections does not allow a correct modeling of the low-temperature part of the TDLS curve, which is dominated by the electron capture time constant $\tau_{n0}(T) \propto 1/\sigma_n(T)$. This explains the strong dependence of the fitted defect parameters on the lower bound of the fitting region: the energy level $E_C - E_t$ ranges, e.g., from 0.40 to 0.44 eV when the lower bound is moved from 270 K (−3 °C) to 310 K (37 °C). Nevertheless, an adequate fit of the position and slope of the Arrhenius increase is only achieved for a defect in the band-gap half close to the minority band (MinBH: upper half in *p*-type), while a reasonable simulation with a defect in the band-gap half close to the majority band (MajBH: lower half in *p*-type) fails.

Among the different models for carrier capture reported in literature the observed decrease of the capture cross section with increasing temperature is only found for an attractive Coulomb center, which can be described in terms of $\sigma(T) = \sigma_0 T^{\alpha}$ with $\alpha < 0$. As all investigated Cz-Si samples with base resistivities from 0.5 to 3.5 Ω cm showed the same temperature dependence in the low temperature region with exponents α varying from −1.5 to −2.0, it can definitely be concluded that the Cz-specific defect in the active state acts as attractive Coulomb center. This finding explains the extreme recombination activity observed for the Cz-specific defect.

If this $\sigma(T)$-model with $\alpha = -2.0$ is introduced into the SRH analysis, an accurate simulation is achieved for a MinBH-defect in the upper band-gap half, which leads to $E_C - E_t = 0.426$ eV and $k = 15.2$ (solid line in Fig. 1). As the SRH simulation for a MajBH defect with the same energy depth $E_V - E_t = 0.426$ eV completely fails for arbitrary k (dashed line in Fig. 1 for $k = 1$), the energy level of the Cz-specific defect in the active state can definitely be localized in the upper band-gap half.

In order to quantify the accuracy of the determined defect parameters, two effects have to be considered: (i) the tolerance of the fitting model towards slight fluctuations of the fitting parameters and (ii) the remaining uncertainty in the slope of the Arrhenius increase, due to the superposed defect annihilation.

In order to quantify the first effect, we simulated the TDLS curve for a variation of energy levels $E_C - E_t$ and determined the optimal k factor for each $E_C - E_t$ from a least-squares fit on the measured TDLS curve for fixed energy level. The resulting symmetry factors k_{opt} and the corresponding least-squares errors are displayed in the upper and the lower half of Fig. 2, respectively, as a function of the energy level $E_C - E_t$ (closed circles). Both curves together represent the *defect parameter solution surface* (DPSS) of the TDLS curve. If a least-squares error which is increased by a factor of 2 above its optimal value of 7.1×10^{-2} is defined as tolerable, the following ranges of acceptable values for the defect parameters can be deduced from the DPSS diagram: $E_C - E_t = 0.39 - 0.46$ eV and $k = 6.2 - 36$.

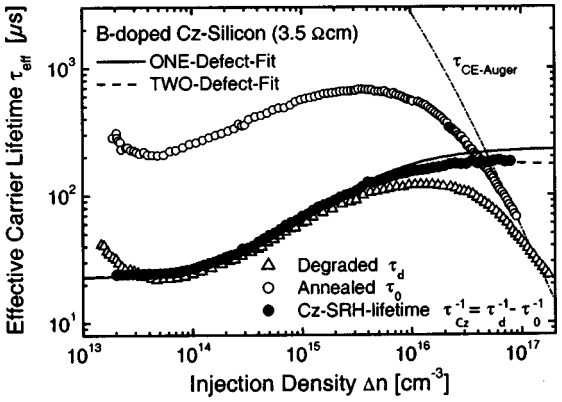

FIG. 3. IDLS curves measured by means of the QSSPC method on the boron-doped Cz-sample investigated in Fig. 1 after annealing at 425 °C for 25 min (τ_0, open circles) and after degradation for 36 h under AM1.5 (intensity 100 mW/cm^2) (τ_d, open triangles). The solid and dashed line represent SRH simulations of the injection dependence of the difference curve τ_{Cz} (solid circles) assuming one and two defect levels, respectively.

In order to quantify the second effect, an additional set of DPSS curves was determined in which the upper bound for the TDLS fit was reduced from 520 K (247 °C) (closed circles in Fig. 2) to 460 K (187 °C) (closed triangles in Fig. 2). This change ensures that only lifetime values are included in the fit which are definitely free from defect annihilation (see above). The best fit is achieved for a MinBH defect with slightly decreased defect parameters $E_C-E_t=0.414$ eV and $k=10.3$. As expected, the Chi^2 curve (open triangles) is shifted to lower values and becomes flatter. This is reflected in a slight broadening of the acceptable range for the defect parameters: $E_C-E_t=0.37-0.46$ eV and $k=3.3-37$.

In order to verify the results obtained from TDLS analysis, an IDLS experiment was performed on the same Cz-sample investigated with the help of TDLS. Figure 3 displays the IDLS curves measured by means of the QSSPC method after an annealing step of 25 min at 425 °C in forming gas (τ_0, open circles) and after an illumination step of 36 h under AM1.5 (intensity 100 mW/cm^2) (τ_d, open triangles), respectively. The IDLS analysis is performed on the quantity $(1/\tau_d-1/\tau_0)^{-1}$ (closed circles). The stability of the surface recombination velocity was controlled on a silicon-nitride-passivated high purity float zone silicon control wafer whose carrier lifetime did not notably change upon the illumination/annealing cycle. Assuming that all additional recombination centers within the Cz-Si wafer are not affected by the illumination/annealing cycle, the quantity $(1/\tau_d-1/\tau_0)^{-1}$ equals the SRH-lifetime τ_{Cz} of the Cz-specific defect in the active state. Note, that this evaluation scheme also eliminates the influence of all intrinsic recombination channels such as Auger and radiative recombination.

Up to $\Delta n=10^{16}$ cm^{-3} the injection dependence of the difference curve τ_{Cz} can be simulated accurately with one single defect level (solid line in Fig. 3), whereas the simulation of the complete curve requires the introduction of a second shallow defect level (dashed line). The existence of such a shallow level activated by illumination was also observed on some of the Cz samples investigated by Schmidt *et al.*[2] But as TDLS is performed under LLI conditions, only the deep center dominating the injection range up to 10^{16} cm^{-3} is relevant for the comparison of IDLS and TDLS.

It must be emphasized that the SRH parameterization of the IDLS curve is not unambiguous. Thus, a detailed analysis of the IDLS data requires determining the *defect parameter solution surface* for the IDLS curve (see above). The resulting k_{opt}- and Chi^2-curve are displayed in Fig. 2 (open squares) together with the corresponding curves for the TDLS data (closed symbols). A fundamental difference between the DPSS curves developed from the TDLS and IDLS data can be observed: while the Chi^2-curves of the TDLS fits (closed symbols) show a pronounced minimum which indicates the best parameterization (E_C-E_t,k), the Chi^2 curve of the IDLS curve (open squares) is totally constant over a broad range of energy levels which shows that the defect parameters *cannot* be determined from only one IDLS curve.

Beyond the instructive illustration of the SRH simulation the combined DPSS diagram, which contains the DPSS curves of the TDLS *and* the IDLS measurement on the investigated Cz-Si sample, allows an accurate determination of the defect parameters of the Cz-specific defect from the intersection point of the k_{opt} curves obtained for the IDLS and TDLS measurement. The Cz-specific defect can be localized in the upper half of the band gap at $E_C-E_t=0.410$ eV showing an electron/hole capture cross section ratio $k=9.3$.

The quality of this finding is manifested in the coincidence of the intersection point of the two $k_{opt}(E_C-E_t)$ curves with the minimum of the $Chi^2(E_C-E_t)$ curve obtained for the TDLS fit with reduced upper temperature limit (closed triangles). This demonstrates in retrospect that the defect annihilation could be absolutely suppressed at least up to 190 °C. The strength of the current determination is that two independent methods lead to the same result: TDLS alone *and* the combination of TDLS and IDLS. This demonstrates the excellent performance of both lifetime spectroscopic methods.

The authors would like to acknowledge the funding by the German Ministry of Education and Research BMBF (Contract No. 01SF0010).

[1] S. W. Glunz, S. Rein, J. Y. Lee, and W. Warta, J. Appl. Phys. **90**, 2397 (2001).
[2] J. Schmidt and A. Cuevas, J. Appl. Phys. **86**, 3175 (1999).
[3] S. Rein, T. Rehrl, W. Warta, S. W. Glunz, and G. Willeke, in *Proceedings of the 17th European Photovoltaic Solar Energy Conference, Munich, Germany* (WIP, Munich, 2002), p. 1555.
[4] J. Schmidt, K. Bothe, and R. Hezel, in *Proceedings of the 29th IEEE Photovoltaics Specialists Conference, New Orleans, LA* (IEEE, New York, 2002).
[5] S. Rein, T. Rehrl, W. Warta, and S. W. Glunz, J. Appl. Phys. **91**, 2059 (2002).
[6] W. Shockley and W. T. J. Read, Phys. Rev. **87**, 835 (1952).
[7] R. N. Hall, Phys. Rev. **87**, 387 (1952).
[8] S. Rein, P. Lichtner, W. Warta, and S. W. Glunz, in *Proceedings of the 29th IEEE Photovoltaics Specialists Conference, New Orleans, LA* (IEEE, New York, 2002).
[9] R. A. Sinton and A. Cuevas, Appl. Phys. Lett. **69**, 2510 (1996).
[10] H. Mäckel and R. Lüdemann (unpublished).